

**Review and Analysis of the Davis-Besse
March 2002 Reactor Pressure Vessel Head
Wastage Event**

Prepared for

First Energy Nuclear Operating Corporation
c/o Morgan Lewis
1111 Pennsylvania Avenue, NW
Washington, DC 20004

Prepared by:

Exponent Failure Analysis Associates
21 Strathmore Road
Natick, MA 01760

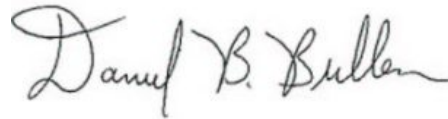
Altran Solutions Corporation
451 D Street
Boston, MA 02210

December 15, 2006

© Exponent, Inc.



Ronald M. Latanision, Ph.D.



Daniel B. Bullen, Ph.D., P.E.



Ronald Ballinger, Ph.D.

Contents

	<u>Page</u>
List of Figures	vi
List of Tables	xiii
Acronyms and Abbreviations	xiv
1 Introduction, Purpose and Scope	1-1
2 Principal Conclusions and Opinions	2-1
3 Background	3-1
3.1 Overview of the Davis-Besse Plant	3-1
3.2 The Davis-Besse Reactor Pressure Vessel Head	3-2
3.3 The Davis-Besse CRDM Nozzles	3-2
3.4 References	3-16
4 The Davis-Besse March 2002 Event	4-1
4.1 Summary Chronology of the March 2002 Event	4-1
4.1.1 RPV Head Video Inspections, CRDM Flange Leakage, Boric Acid Deposits, and Head Cleaning	4-2
4.1.2 CRDM Nozzle UT Inspections	4-3
4.2 March 2002 13RFO Discovery of Large Head Corrosion Cavity at CRDM Nozzle 3 and Minor Crevice Corrosion at CRDM Nozzle 2 in the RPV Head	4-4
4.2.1 Initial Discovery of the Corrosion Cavity in the Reactor Pressure Vessel Head	4-5
4.2.2 Inspection and Metallurgical Analysis of the Nozzles and Corrosion Cavity	4-6
4.3 Responses to the March 2002 Davis-Besse RPV head Corrosion Cavity Discovery	4-6
4.3.1 FENOC Responses	4-7
4.3.2 EPRI Material Reliability Program (MRP) Response	4-14
4.3.3 Regulatory Response	4-15
4.4 References	4-32
5 Worldwide Industry Response to CRDM and Other Alloy 600 Nozzle Cracking	5-1
5.1 Non-US Experience with and Responses to CRDM Nozzle Cracking	5-2
5.1.1 Bugey-3 and Subsequent EdF Experience	5-2

	5.1.2	Other Non-US Experience with CRDM Nozzle Cracking	5-5
5.2		Alloy 600 Pressurizer Nozzle Cracking	5-8
5.3		US Experience with and Responses to CRDM Nozzle Cracking	5-10
	5.3.1	Initial Experience of CRDM Nozzle Inspections and Cracking in US Plants 1994-2000	5-10
	5.3.2	Initial US Industry and NRC Regulatory Response to CRDM Nozzle Cracking	5-14
	5.3.3	NRC/INEL/EG&G Assessment of CRDM Nozzle Cracking	5-21
	5.3.4	NRC Generic Letter GL 97-01 and Industry Response	5-23
	5.3.5	Experience of CRDM Nozzle Cracking in US	5-27
	5.3.6	US Industry and NRC Regulatory Response to CRDM Nozzle Cracking 2000-2001	5-33
	5.3.7	US CRDM Nozzle Cracks, Repairs, and RPV Head Replacements Since 2000	5-36
5.4		References	5-44
6		Boric Acid Wastage of Carbon Steel Components in US PWR Plants	6-1
	6.1	Review of US Experience with Boric Acid Corrosion of Carbon Steel Components Prior to 2002	6-4
	6.1.1	Boric Acid Corrosion of Components Other than the RPV Head	6-4
	6.1.2	Boric Acid Corrosion of RPV and Pressurizer heads Prior to the 2002 Davis-Besse Event	6-10
	6.2	NRC Regulatory and US Industry Responses to Boric Acid Corrosion Issues 1980-2001	6-14
	6.3	Boric Acid Corrosion Research and Testing Prior to 2002	6-20
	6.3.1	Non-Crevice Geometry Boric Acid Corrosion Testing	6-20
	6.3.2	Crevice Geometry Boric Acid Corrosion testing Prior to 2002	6-24
	6.4	Recent Research on Boric Acid Corrosion of RPV Head Resulting from the Davis-Besse Event	6-28
	6.4.1	EPRI Boric Acid Corrosion testing to Replicate the Davis-Besse RPV Head Wastage Event	6-28
	6.4.2	NRC/ANL Corrosion Test Programs to Replicate the Davis-Besse Wastage Conditions	6-32
	6.5	References	6-50
7		FENOC/Davis-Besse Response to CRDM Cracking and Boric Acid Corrosion Issues	7-1
	7.1	Davis-Besse Action and Responses to Key US NRC and Industry Initiatives	7-2

	7.1.1	Davis-Besse Response to NRC Bulletin 88-05 and the Implementation of a Boric Acid Corrosion Control Program	7-3
	7.1.2	FENOC Responses to US NRC Bulletin 2001-01 and Subsequent Information Requests	
7.2		RCS Leakage Monitoring at Davis-Besse	7-17
	7.2.1	RCS Inventory Balance	7-17
	7.2.2	RB Radiation Monitoring	7-19
7.3		Review of Davis-Besse Plant Refueling Outages and History of Boric Acid Leakage	7-21
	7.3.1	Pre-8RFO CRDM Flange Leakage	7-21
	7.3.2	8RFO Inspections and Events – March/April 1993	7-22
	7.3.3	9RFO Inspections and Events – October/November 1994	7-22
	7.3.4	10RFO Inspections – April/May 1996	7-23
	7.3.5	11RFO Inspections – April/May 1998	7-23
	7.3.6	12RFO Inspections, Events and NRC Regulatory Review – April/May 2000	7-26
	7.3.7	13RFO Inspections – Started February 2002	7-28
7.4		References	7-48
8		Stress Analysis and Crack Growth Rates for Davis-Besse CRDM Nozzles 2 and 3	8-1
	8.1	PWSCC and Prior Industry Stress Analysis Studies	8-2
	8.1.1	PWSCC of Alloy 600 Materials in PWRs	8-2
	8.1.2	Prior Industry Stress Analysis Studies	8-5
	8.2	Stress Analysis of Davis-Besse CRDM Nozzles 2 and 3	8-5
	8.2.1	Finite Element Model of CRDM Nozzle 3 Head Penetration	8-6
	8.2.2	Material Properties	8-7
	8.2.3	Loading Conditions	8-8
	8.2.4	Stress Analysis Results	8-9
	8.3	PWSCC Crack Growth Rates for Davis-Besse CRDM Nozzles	8-10
	8.3.1	Crack Growth Rates Used in Previous Work	8-10
	8.3.2	Recent Data on Davis-Besse Nozzle and Weld Alloy 600/182 Materials by NRC/ANL	8-12
	8.4	PWSCC Cracks in Davis-Besse CRDM Nozzles 2 and 3	8-15
	8.4.1	Effective Crack Leak Lengths of the Axial PWSCC Cracks in Nozzles 2 and 3	8-15
	8.4.2	Reconstruction of the Crack 1 Profile in RDM Nozzle 3 and J-groove Weld	8-16
	8.5	Crack Growth Rates for Observed Cracks at Davis-Besse CRDM Nozzles 2 and 3	8-17
	8.5.1	Estimate of Time at Which Cracks in CRDM Nozzles 2 and 3 Reached Through Wall above Weld and Leakage Began	8-17

	8.5.2	The Unique Nature of the Cracking at Nozzle 3	8-20
8.6		References	8-34
9		CFD Modeling of Fluid Flow in CRDM Nozzle and Weld Cracks and Through Annulus	9-1
	9.1	Prior Assessments of Thermal Hydraulic Environments in the CRDM Annulus and Developing Wastage Cavity	9-2
	9.2	RPV Head Low Alloy Steel Removal Mechanisms and Wastage Rates	9-8
	9.3	Approach to CFD Modeling and Model Development	9-10
		9.3.1 Overall Approach to CFD Modeling	9-10
		9.3.2 CFD Model Development	9-11
	9.4	Leak Rate vs. Crack Length Calculations	9-13
	9.5	Development of the Initial Wastage Cavity in the CRDM Nozzle Annulus	9-16
	9.6	CFD Modeling of the Initial Stages of Wastage Cavity Growth at CRDM Nozzles 2 and 3	9-19
		9.6.1 Input and Boundary Conditions	9-20
		9.6.2 CFD Case 1—Crack Length of 0.5 Inch, Leak Rate of 0.001 gpm, Bottom of Wastage Cavity 2 Inches Above Top of Crack	9-24
		9.6.3 CFD Case 2—Crack Length of 0.8 Inch, Leak Rate of 0.01 gpm, Bottom of Wastage Cavity 1.7 Inches Above Top of Crack	9-26
		9.6.4 CFD Case 3—Crack Length of 1.0 Inch, Leak Rate of 0.02 gpm, Bottom of Wastage Cavity 0.2 Inches Below Top of Crack	9-29
	9.7	CFD Modeling of the Final Wastage Cavity at CRDM Nozzle 3	9-31
		9.7.1 CFD Case 4—Modeling of the Final Wastage Cavity at CRDM Nozzle 3 and Final Leak Rate in February 2002	9-31
		9.7.2 CFD Case 5—Transient Analysis of Fluid Flow and Fluid Ejection from the Final Wastage Cavity at CRDM Nozzle 3	9-33
	9.8	Summary	9-35
	9.9	References	9-67
10		Development of Wastage Cavities at Davis-Besse CRDM Nozzles 2 and 3	10-1
	10.1	Wastage Cavities at Nozzles 3 and 2	10-2
		10.1.1 Physical Appearance and Characteristics of the Wastage Cavity at Nozzle 3	10-2
		10.1.2 Physical Appearance and Characteristics of the Wastage Cavity at Nozzle 2	10-3
		10.1.3 Cracks in CRDM Alloy 600 Nozzle 3 and Alloy 182 Weld	10-4

	10.1.4	Metal Removal Processes by Corrosion, Erosion, Flow Assisted Corrosion (FAC), and Water Jet Cutting	10-5
10.2		Timeline of Cavity Development at Nozzles 3 and 2	10-6
	10.2.1	12 RFO: Nozzle 3 Crack is Leaking at a Low Rate And a Minor Wastage Cavity Begins to Form at Nozzle 3	10-7
	10.2.2	October-November 2001: Weld Crack Uncovers, Leak Rate Dramatically Increases, Cavity Growth Accelerates, and Significant Damage to the RPV Head Occurs	10-9
10.3		Postscript	10-11
10.4		References	10-28
Appendix A		Finite Element Stress Analysis of Davis-Besse CRDM Nozzle 3 Penetration	
Appendix B		Crack Driving Force and Growth Rate Estimates	
Appendix C		CFD Analysis	
Appendix D		Leak Rate vs. Crack Length Calculations	
Appendix E		Fluid Jet Cutting of Davis-Besse RPV Head Materials	

List of Figures

		<u>Page</u>
Figure 3.1	Davis-Besse NSSS Showing “Raised Loop” Configuration	3-5
Figure 3.2	Typical Reactor Pressure Vessel Head General Arrangement	3-6
Figure 3.3	Davis-Besse Reactor Pressure Vessel Head Sectional View	3-7
Figure 3.4	Davis-Besse Reactor Pressure Vessel Head Sectional View	3-8
Figure 3.5	Davis-Besse Reactor Pressure Vessel Head Plan View	3-9
Figure 3.6	View of the Underside of the Davis-Besse RPV Head with Control Rods in Place	3-10
Figure 3.7	View through the Access Opening Cut in the RPV head Service Structure above the Support Steel and Insulation Showing the Close Proximity of the CRDM Flanges	3-11
Figure 3.8	View through the Access Opening Cut in the RPV Head Service Structure above the Support Steel and Insulation Showing the Close Proximity of the CRDM Flanges	3-12
Figure 3.9	Davis-Besse CRDM Nozzle General Arrangement	3-13
Figure 4.1	Boric acid and iron oxide flowing from mouse holes at 12RFO.	4-23
Figure 4.2	Davis-Besse RPV head wastage cavity found adjacent to Nozzle 3.	4-24
Figure 4.3	Location of RPV head wastage on the downhill side of Nozzle 3.	4-25
Figure 4.4	Crevice identified by inspection of Nozzle 2 with a hand-held video camera following the removal of a section of mirror insulation.	4-26
Figure 4.5	Portion of the J-groove weld with the 10-degree crack.	4-27
Figure 4.6	J-groove weld with the 10-degree crack showing crack and flow channel.	4-28
Figure 4.7	Surface morphology of the Davis-Besse RPV head wastage cavity looking toward the nose of the cavity (~10-degree).	4-29
Figure 4.8	Surface morphology of the Davis-Besse RPV head wastage cavity looking toward the 90-degree side.	4-30
Figure 4.9	Surface morphology of the Davis-Besse RPV head wastage cavity looking toward the 270-degree side.	4-31

Figure 6.1	Areas on the RPV Head at Turkey Point-4 Affected by Boric Acid Wastage in 1987 (from EPRI Boric Acid Corrosion Guidebook, April 1995)	6-37
Figure 6.2	Effect of Boric Acid Deposits in Protecting Surfaces from Corrosion (from EPRI Boric Acid Corrosion Guidebook, April 1995)	6-38
Figure 6.3	Boric Acid Corrosion Test Program Configurations and Conditions (from EPRI Boric Acid Corrosion Guidebook, April 1995)	6-39
Figure 6.4	Summary of Boric Acid Corrosion Test Results (from EPRI Boric Acid Corrosion Guidebook, Revision 1, November 2001)	6-40
Figure 6.5	Temperature Dependency of Corrosion Rate in B & W Tests of Water Containing Boric Acid Dripping onto Pipes (from EPRI Boric Acid Corrosion Guidebook, Revision 1, November 2001)	6-41
Figure 6.6	CE Crevice Test Configuration for Boric Acid Leakage into an Annular Crevice (from EPRI Boric Acid Corrosion Guidebook, Revision 1, November 2001)	6-42
Figure 6.7	Location of Wastage in CE Crevice Test Configuration for Boric Acid Leakage into an Annular Crevice (from EPRI Boric Acid Corrosion Guidebook, Revision 1, November 2001)	6-43
Figure 6.8	EPRI Crevice Test Configuration for Boric Acid Leakage into an Annular Crevice (from EPRI Boric Acid Corrosion Guidebook, Revision 1, November 2001)	6-44
Figure 6.9	Maximum Wastage Rates from CE and EPRI Crevice Test Results (from EPRI Boric Acid Corrosion Guidebook, Revision 1, November 2001)	6-45
Figure 6.10	Typical Corrosion/Erosion Wastage Pattern Near Injection Point in EPRI Crevice Test for Boric Acid Leakage into an Annular Crevice (Slide 26 from the May 22, 2002 EPRI Meeting with the NRC; also in EPRI Boric Acid Corrosion Guidebook, Revision 1, November 2001)	6-46
Figure 6.11(a)	EPRI MRP Corrosion Testing Wastage Model: Phase 1 and Phase 2	6-47
Figure 6.11(b)	EPRI MRP Corrosion Testing Wastage Model: Phase 3 and Phase 4	6-48
Figure 7.1	Daily average unidentified leak rate for Davis-Besse Cycle 13.	7-31
Figure 7.2	Three-day average unidentified leak rate for Davis-Besse Cycle 13.	7-32

Figure 7.3	Thirty-day average unidentified leak rate for Davis-Besse Cycle 13.	7-33
Figure 7.4	Monthly average unidentified leak rate for Davis-Besse Cycles 10 through 13.	7-34
Figure 7.5	Location of radiation monitors RE 4597AA and RE 4597BA.	7-35
Figure 7.6	Noble gas activity for Cycles 10-13 for radiation monitors RE 4597AA and RE4597BA.	7-36
Figure 7.7	Iodine activity for Cycles 10-13 for radiation monitors RE4597AA and RE4597BA.	7-37
Figure 7.8	Flange Leakage Showing Boric Acid Deposits Leaking Through the Mirror Insulation at 8RFO.	7-38
Figure 7.9	Flange Leakage Showing Boric Acid Deposits On Side of Nozzles and Stalactites from Gaps in Insulation (8RFO).	7-39
Figure 7.10	Reddish Brown Boron Deposits Crusted on Side of Nozzle (8RFO).	7-40
Figure 7.11	Boric Acid Deposits behind the CRDM Nozzles on the North Side of the Reactor Pressure Vessel Head at 10RFO.	7-41
Figure 7.12	Boron Piled on Reactor Pressure Vessel Head Under the Mirror Insulation Near Nozzle 31 (11RFO).	7-42
Figure 7.13	Boron Piled Up to the Mirror Insulation Near the Center of the RPV Head (12RFO).	7-43
Figure 7.14	Boric Acid Deposits on RPV head at 13RFO. Note this is Figure 24 from the Root Cause Report.	7-44
Figure 7.15	Corrosion Product/Boric Acid Deposits Adjacent to Nozzle 3 (90 Degree Side) after Hydrolasing.	7-45
Figure 7.16	Corrosion Product/Boric Acid Deposits Adjacent to Nozzle 3 (270 Degree Side) after Hydrolasing.	7-46
Figure 8.1	Crack initiation and growth in steam generator tubes, (a) lab-generated SCC cracks showing multiple crack initiation; (b) actual steam generator tube crack; (c) eddy current inspection signal from the tube crack in (b) one cycle earlier	8-22
Figure 8.2	Three-dimensional, half-symmetry finite element model of CRDM Nozzle-3 head penetration, showing Alloy-600 nozzle, Alloy-182 J-groove weld, and surrounding SA-533 alloy steel head with Type 308 stainless steel cladding	8-23

Figure 8.3	Close-up view of 13-pass J-groove weld joining CRDM Nozzle 3 to alloy-steel head.	8-23
Figure 8.4	PWSCC growth rate data for Alloy 600 from Davis-Besse Nozzle 3 compared to EPR/MRP disposition curve.	8-24
Figure 8.5	Nozzle-circumferential (hoop) stress results in ksi for downhill side of Nozzle 3 at J-groove weld under operating pressure and temperature (2,155 psi, 605°F).	8-25
Figure 8.6	Nozzle-axial stress results in ksi for downhill side of Nozzle 3 at J-groove weld under operating pressure and temperature (2,155 psi, 605°F).	8-26
Figure 8.7	Framatome plot of crack profiles in Davis-Besse CRDM Nozzle 2 based on UT results	8-27
Figure 8.8	Through-wall profile of Crack in Davis-Besse CRDM Nozzle 2 based on Framatome UT results.	8-28
Figure 8.9	PWSCC growth rate for Alloy 182 from Davis-Besse Nozzle 11J-groove weld compared to EPR/MRP disposition curve.	8-29
Figure 8.10	Through-wall profile of Crack in Davis-Besse CRDM Nozzle 2 based on Framatome UT results.	8-30
Figure 8.11	BWXT photographs from metallurgical examination of Davis-Besse Nozzle-3 J-groove weld showing extent of PWSCC Crack 1 into weld.	8-31
Figure 8.12	Schematic of final size and shape of Crack 1 in Davis-Besse CRDM Nozzle 3 developed from Framatome UT test records and BWXT metallurgical sections.	8-32
Figure 9.1(a)	CFD Model Mesh for Case 3 Small Wastage Cavity	9-36
Figure 9.1(b)	CFD Model Mesh for Case 3 Small Wastage Cavity	9-37
Figure 9.2(a)	CFD Model Mesh for Case 4 Large Wastage Cavity	9-38
Figure 9.2(b)	CFD Model Mesh for Case 4 Large Wastage Cavity	9-39
Figure 9.3	Calculated Leak rate vs. Crack Length Above the J-Groove Weld as Calculated by Dominion Engineering, Inc.	9-40
Figure 9.4	CRDM Nozzle Leak Rate vs. Crack Height	9-41
Figure 9.5	Scanning electron micrograph of CRDM Nozzle 3 crack at 180° location showing typical dimensions of PWSCC nozzle crack widths. Note the maximum crack width is about 20 μm (0.0008 inches).	9-42

Figure 9.6	Optical micrograph of J-groove weld crack in CRDM Nozzle 3 at 10° location showing large crack width. Note the nominal crack width is about 400 μm (0.016 inches) or about 20 times larger than the PWSCC crack in the same nozzle shown above.	9-42
Figure 9.7	Calculated leak rate vs. crack length for a J-groove weld crack with crack widths that are 10 times, 15 times, and 20 times wider than typical PWSCC nozzle cracks.	9-43
Figure 9.8	Case 1: Maximum and average fluid velocity magnitude within wastage as a function of distance to the J-groove weld for a 0.5-inch crack with a leak rate of 0.001 gpm.	9-44
Figure 9.9	Case 1: Average fluid pressure within wastage as a function of distance to the J-groove weld for a 0.5-inch crack with a leak rate of 0.001 gpm.	9-45
Figure 9.10	Case 1: Average wall temperature within wastage as a function of distance to the J-groove weld for a 0.5-inch crack with a leak rate of 0.001 gpm.	9-46
Figure 9.11	Case 1: Average steam quality within wastage as a function of distance to the J-groove weld for a 0.5-inch crack with a leak rate of 0.001 gpm.	9-47
Figure 9.12	Case 2: Maximum and average fluid velocity magnitude within wastage as a function of distance from the J-groove weld for a 0.8-inch crack with a leak rate of 0.01 gpm.	9-48
Figure 9.13	Case 2: Average fluid pressure within wastage as a function of distance to the J-groove weld for a 0.8-inch crack with a leak rate of 0.01 gpm.	9-49
Figure 9.14	Case 2: Average wall temperature within wastage as a function of distance to the J-groove weld for a 0.8-inch crack with a leak rate of 0.01 gpm.	9-51
Figure 9.15	Case 2: Average steam quality within wastage as a function of distance to the J-groove weld for a 0.8-inch crack with a leak rate of 0.01 gpm.	9-51
Figure 9.16	Case 3: Maximum and average fluid velocity magnitude within wastage as a function of distance to the J-groove weld for a 1.0-inch crack with a leak rate of 0.02 gpm.	9-52
Figure 9.17	Case 3: Average fluid pressure within wastage as a function of distance to the J-groove weld for a 1.0-inch crack with a leak rate of 0.02 gpm.	9-53

Figure 9.18	Case 3: Average temperature within wastage as a function of distance to the J-groove weld for a 1.0-inch crack with a leak rate of 0.02 gpm.	9-54
Figure 9.19	Case 3: Average steam quality within wastage as a function of distance to the J-groove weld for a 1.0-inch crack with a leak rate of 0.02 gpm.	9-55
Figure 9.20	Velocity magnitude contours for the final wastage state sectioned directly through crack. The viewpoint is looking up from below RPV head.	9-56
Figure 9.21	Temperature contours for the final wastage state sectioned directly through crack. The viewpoint is looking up from below RPV head.	9-57
Figure 9.22	Cavity wall temperature contours for the final wastage state. The viewpoint is looking up from below RPV head from a different orientation than Figures 9.17 and 9.18 to show the cavity wall temperatures directly opposite the cracks.	9-58
Figure 9.23	Top View of Wastage Cavity on Davis-Besse RPV Head.	9-59
Figure 9.24	Wastage Cavity Sidewalls Viewed at Low Magnification Looking Toward 90° and 270°.	9-60
Figure 9.25(a)	Dental Mold of Wastage Cavity Looking Towards 0° and 90°.	9-61
Figure 9.25(b)	Dental Mold of Wastage Cavity Looking Towards 180° and 270°.	9-62
Figure 9.26	Transient analysis results for final wastage cavity filled with boric acid solution for time steps from 0.001 seconds to 0.02 seconds.	9-63
Figure 9.27	Transient analysis results for final wastage cavity filled with boric acid solution for time steps from 0.05 seconds to 0.10 seconds.	9-64
Figure 9.28	Transient analysis results for final wastage cavity filled with boric acid solution for time steps from 0.12 seconds to 0.20 seconds.	9-65
Figure 9.29	Transient analysis results for final wastage cavity filled with boric acid solution for time steps from 0.25 seconds to 0.40 seconds.	9-66
Figure 10.1	Top View of wastage cavity	10-13
Figure 10.2	View of cavity looking toward 270°	10-14
Figure 10.3	View of cavity looking toward 90°	10-15

Figure 10.4	Low magnification photographs of cavity sidewalls	10-16
Figure 10.5(a)	Photographs of cavity dental mold	10-17
Figure 10.5(b)	Photographs of cavity dental mold	10-18
Figure 10.6	Wastage Cavity at CRDM Nozzle 2	10-19
Figure 10.7	Wastage Cavity at CRDM Nozzle 2	10-20
Figure 10.8	Schematic of final size and shape of Crack 1 in Davis-Besse CRDM Nozzle 3 (from Section 8, Figure 8.10)	10-21
Figure 10.9	PT results for nozzle 3 J-groove weld bore and cladding underside. The J-groove weld contained an axial indication near 10°	10-22
Figure 10.10	Photograph showing the remaining portion of the axial crack near 10° in the CRDM Nozzle 3 J-groove weld. This is the portion remaining after the machining was completed for nozzle repair.	10-23
Figure 10.11	Photograph showing axial crack in CRDM nozzle 3 J-groove weld near 10°.	10-24
Figure 10.12	Piece A2A6 was first sectioned into Pieces A2A6A and A2A6B. Piece A2A6A was further sectioned into Pieces A2A6A1 and A2A6A2. Both cuts were made on the same plane, parallel to the paper. The first cut line is partially visible; Piece A2A6B is the upper portion of the weld. The second cut line between Pieces A2A6A1 and A2A6A2 is obscured by Piece A2A6A1	10-25
Figure 10.13	Piece A2A6B after sectioning. The bottom surface of A2A6B2 was mounted. The axial crack in A2A6B3 was opened up for SEM.	10-26
Figure 10.14	Macro photograph of metallographic mount sample A2A6B2 (see Figures 5.4 and 5.5 for the sample orientation). The axial cracking at ~10o is through the J-groove weld, in contrast to the cracking near 180o, which was partially through the weld. A slightly higher magnification micrograph is also provided	10-27

List of Tables

		<u>Page</u>
Table 3.1	Principal Design Parameters of the Davis-Besse Plant	3-14
Table 3.2	Davis-Besse CRDM Nozzle Geometry, Materials and Operating Parameters	3-15
Table 5.1	EdF CRDM Inspection Results Reported at the 1992, 1994, and 2000 EPRI Workshops on PWSCC	5-38
Table 5.2	Summary of US Plants with Detected RPV Head CRDM Nozzle and/or Weld Cracking (from MRP-110)	5-39
Table 5.3	Orientation and Location of CRDM Nozzle Cracks in US Plant RPV Head CRDM Nozzles (from MRP-110)	5-40
Table 5.4	Summary of Inspections of US Plant RPV Head Nozzle J-Groove Welds (from MRP-110)	5-41
Table 5.5	Summary of US Plants with Detected RPV Head CRDM Nozzle Leakage (from MRP-110)	5-42
Table 5.6	Summary of US Plant RPV Head Replacements (from MRP-110)	5-43
Table 6.1	Test Parameters and Wastage Results from CE Crevice Test for Boric Acid Leakage into an Annular Crevice (from EPRI Boric Acid Corrosion Guidebook, Revision 1, November 2001)	6-49
Table 6.2	Test Parameters and Wastage Results from EPRI Crevice Test for Boric Acid Leakage into an Annular Crevice (from EPRI Boric Acid Corrosion Guidebook, Revision 1, November 2001)	6-49
Table 7.1	Summary of Identified Leaking CRDM Nozzles and Repairs for 6RFO to 12RFO	7-47
Table 8.1	Axial PWSCC Crack Dimensions in Davis-Besse CRDM Nozzle 2 for Cracks Extending Above the Top of the J-groove Weld	8-33
Table 8.2	Axial PWSCC Crack Dimensions in Davis-Besse CRDM Nozzle 3 for Cracks extending Above the Top of the J-groove Weld	8-33

Glossary of Terms and Abbreviations

ANO-1	Arkansas Nuclear One
AIT	Augmented Inspection Team (NRC)
ANL	Argonne National Laboratory
ANSI	American National Standards Institute
ASME	American Society of Mechanical Engineers
B&W	Babcock & Wilcox
BA	Boric Acid
BAC	Boric Acid Corrosion
BACC	Boric Acid Corrosion Control
BNL	Brookhaven National Laboratory
BWOG	B & W Owners Group
CAC	Containment Air Cooler
CAL	Confirmatory Action Letter
CE	Combustion Engineering
CEOG	CE Owners Group
CFD	Computational Fluid Dynamics
CGR	Crack Growth Rate
CNRB	Company Nuclear Review Board
CR	Condition Report
CRDM	Control Rod Drive Mechanism
CTMT	Reactor Containment
DB	Davis-Besse
DEI	Dominion Engineering Incorporated
ECT	Eddy Current Testing

EdF	Electricité de France
EFPY	Effective Full Power Years
EFPH	Effective Full Power Hours
EPRI	Electric Power Research Institute
FEA	Finite Element Analysis
FENOC	First Energy Nuclear Operating Corporation
FMEA	Failure Mode and Effects Analysis
GAO	US Congress General Accounting Office
GL	Generic Letter (NRC)
gpm	Gallons Per Minute
HVAC	Heating, Ventilation, and Air Conditioning
ID	Inner Diameter
IGA	Inner Granular Attack
ILRT	Integrated Leak Rate Test
IN	Information Notice (NRC)
INPO	Institute for Nuclear Power Operations
ISI	Inservice Inspection
ksi	Kilopounds per Square Inch
LER	Licensee Event Report
LLTF	Lessons Learned Task Force (NRC)
LOCA	Loss of Coolant Accident
MRP	Materials Reliability Program (EPRI)
MWe	Megawatts Electric
NDE	Non-Destructive Examination
NEI	Nuclear Energy Institute

NEIL	Nuclear Electric Insurance Limited
NRC	US Nuclear Regulatory Commission
NRR	Nuclear Reactor Regulation
NSSS	Nuclear Steam Supply System
NUMARC	Nuclear Management and Resource Council
OD	Outer Diameter
PCAQ	Potential Condition Adverse to Quality
psi	Pounds per Square Inch
PT	Dye Penetrant Testing
PWR	Pressurized Water Reactor
PWSCC	Primary Water Stress Corrosion Cracking
QA	Quality Assurance
QC	Quality Control
RAI	Request for Additional Information
RB	Reactor Building
RCPB	Reactor Coolant Pressure Boundary
RCS	Reactor Coolant System
RFO	Refueling Outage
RPV	Reactor Pressure Vessel
SCC	Stress Corrosion Cracking
SIA	Structural Integrity Associates
SWRI	Southwest Research Institute
TECO	Toledo Edison Company
TVA	Tennessee Valley Authority
UT	Ultrasonic Testing

VHP Very High Pressure
WOG Westinghouse Owners Group